ADVANCED QUANTUM TECHNOLOGIES
www.advquantumtech.com

Protocol for Nonlinear State Discrimination in Rotating Condensate

Michael R. Geller

Nonlinear mean field dynamics enables quantum information processing operations that are impossible in linear one-particle quantum mechanics. In this approach, a register of bosonic qubits (such as neutral atoms or polaritons) is initialized into a symmetric product state $|\psi\rangle^{\otimes n}$ through condensation, then subsequently controlled by varying the qubit-qubit interaction. An experimental implementation of quantum state discrimination, an important subroutine in quantum computation, with a toroidal Bose–Einstein condensate is proposed. The condensed bosons here are atoms, each in the same superposition of angular momenta 0 and $\hbar$, encoding a qubit. A nice feature of the protocol is that only a readout of individual quantized circulation states (not superpositions) is required.

1. Introduction

A variety of atomtronic architectures have been proposed for quantum computing and quantum technology applications.[1,2] Two main Bose–Einstein condensate (BEC) types have been considered for realizing qubits: multi-component condensates and multi-mode condensates. Multi-component and spinor condensate approaches[3–8] encode a single qubit in two (or more) metastable atomic states, such as spin or hyperfine levels, with all atoms in the same translational mode (for example the motional ground state). Multi-mode approaches[9–11] encode a single qubit using two (or more) translational modes in a scalar condensate, such as a BEC in a double-well trapping potential. In the limit where there are a large number of condensed bosons in each well, the system becomes equivalent to two (or more) BECs, each with a well-defined phase, connected by tunneling barriers that act as Josephson junctions.[9–11] Arrays of such BECs can be produced in optical lattices and are described by the Bose–Hubbard model.[10,11] Another multi-mode approach, which we adopt here, uses circulating states in a ring geometry[12–18] for the translational modes.

Given the demonstrated high performance and scalability of trapped ion qubits,[19] superconducting qubits,[20–22] and of neutral atom arrays,[23,24] what does a BEC qubit offer? We argue that it offers a platform for an alternative approach to quantum information processing that leverages the special properties of condensates. In this approach, a BEC is used to prepare a register of qubits in a product state $|\psi\rangle^{\otimes n}$ and control its subsequent evolution. From a quantum computing perspective, having multiple identical copies of an *unknown* input is already a useful resource (whereas classical information is freely cloned). In standard circuit-model quantum computation, illustrated in **Figure 1a**, initialized qubits are subsequently entangled using two-qubit gates. Here we do the opposite and try to suppress entanglement, Figure 1b. This is achieved by making n large, interactions weak, and by preserving permutation symmetry. In this limit entanglement monogamy[25,26] bounds the pairwise concurrence to zero, and the BEC is exactly described by a nonlinear Schrödinger equation (the Gross–Pitaevskii equation[27,28]), enabling novel dynamics.[10–12,29–36] The theory is developed in a large n limit with a rigorous bound on the error resulting from the mean field approximation. *The nonlinear approach trades exponential time complexity for space complexity, requiring n to be large.*

Does this mean that n has to be exponentially large? Actually, the requirements on n are not that bad. This is because the BEC is assumed to be initialized in a product state, and it takes time $t_{\rm ent}$ for the atomic collisions to produce entanglement. Ideally, the whole experiment is performed in a short-time regime. We measure the accuracy of mean-field theory by $\epsilon := \|\rho_{\rm eff}(t) - \rho_1(t)\|_1$, and call this the model error. Here $\rho_{\rm eff}$ is the mean-field state, ρ_1 is the exact state traced over all atoms but one, t is the gate duration, and $\|\cdot\|_1$ is the trace norm. In a large family of condensate models[37,38]

$$\epsilon \le c\frac{e^{t/t_{\rm ent}} - 1}{n} \tag{1}$$

where c and $t_{\rm ent}$ are positive constants (model-dependent quantities independent of t and n). Although the error might grow

M. R. Geller
Department of Physics and Astronomy
University of Georgia
Athens, GA 30602, USA
E-mail: mgeller@uga.edu
M. R. Geller
Center for Simulational Physics
University of Georgia
Athens, GA 30602, USA

The ORCID identification number(s) for the author(s) of this article can be found under https://doi.org/10.1002/qute.202300431

DOI: 10.1002/qute.202300431

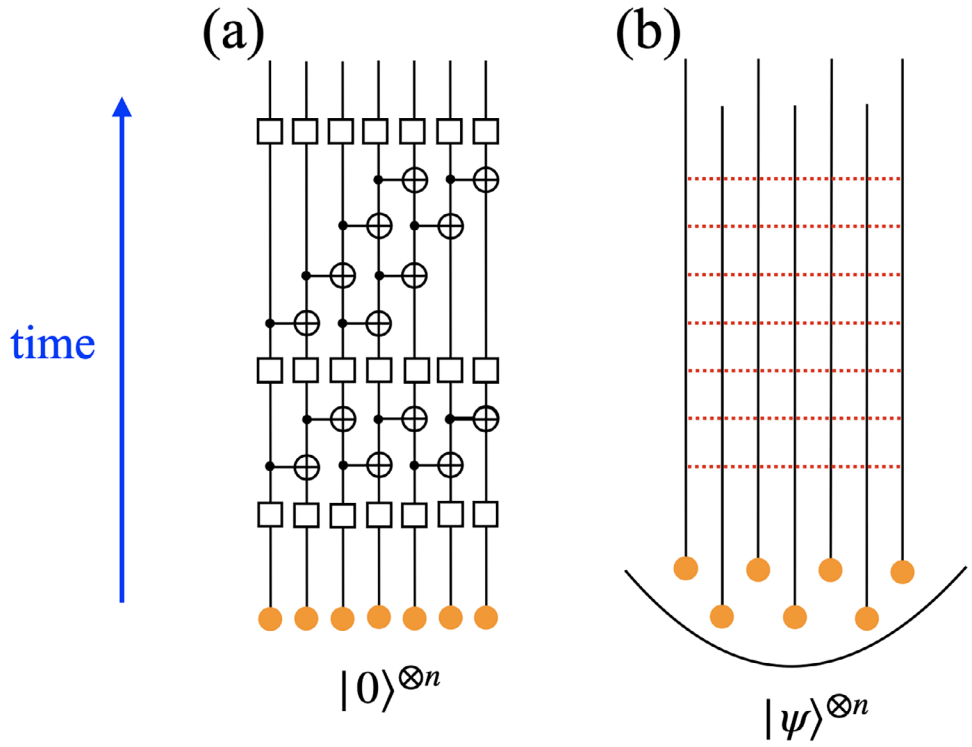

Figure 1. Nonlinear quantum information processing with a BEC. a) In circuit-model quantum computation, a register of qubits is initialized to a product state (such as $|0\rangle^{\otimes n}$), after which gates are applied, entangling the qubits. b) In the nonlinear approach, the qubits ideally remain in a product state $|\psi(t)\rangle^{\otimes n}$ throughout the computation. The BEC simulates a single nonlinear qubit.

exponentially in time, there is always a short-time window $t < t_{\rm ent}$ where the required number of condensed atoms $n \approx ct/t_{\rm ent}\epsilon$ is sub-exponential in t.

We propose a demonstration of quantum information processing using this nonlinearity. In the remainder of this section, we discuss the qubit encoding and state discrimination subroutine. The protocol is explained in Section 2. Conclusions are given in Section 3, and additional information about the BEC model and large n limit are provided in the Appendix.

1.1. Qubit Encoding

BEC-based qubits necessarily encode a small number of parameters ($\psi_{0,1} \in \mathbb{C}$) into a large number of degrees of freedom and the map is not unique. However two encodings can often be considered: Let $a_l^\dagger$ create an atom in BEC component $l \in \{0,1\}$ (in a two-component condensate) or in translational mode $l \in \{0,1\}$ (in a two-mode condensate), and let $\psi_{0,1}$ be complex coordinates satisfying $|\psi_0|^2 + |\psi_1|^2 = 1$. One encoding that is interesting from a quantum foundations perspective is

$$|\mathrm{CAT}_n\rangle := \frac{\psi_0 (a_0^\dagger)^n + \psi_1 (a_1^\dagger)^n}{\sqrt{n!}}|\mathrm{vac}\rangle, \quad \langle \mathrm{CAT}_n|\mathrm{CAT}_n\rangle = 1, \quad n \geq 1 \tag{2}$$

but this is a superposition of two macroscopically distinct BECs (a Schrödinger cat state) which would be highly susceptible to decoherence.[3] Instead, we use the encoding

$$|F_n\rangle := \frac{(\psi_0\, a_0^\dagger + \psi_1\, a_1^\dagger)^n}{\sqrt{n!}}|\mathrm{vac}\rangle, \quad \langle F_n|F_n\rangle = 1, \quad n \geq 1 \tag{3}$$

which is a condensate of n bosons $\psi_0\, a_0^\dagger + \psi_1\, a_1^\dagger$, each a single atom in a superposition of components or modes. (While $|\mathrm{CAT}_n\rangle$ and $|F_n\rangle$ depend on both n and $\psi_{0,1}$, the latter dependence is suppressed.) The encoding (3) was originally proposed by Cirac et al.[3] and by Byrnes et al.[5,6] for two-component condensates; in that case $|F_n\rangle$ is a pseudospin coherent state.[6] But our $a_0^\dagger$ and $a_1^\dagger$ create atoms in circulating states of orbital angular momentum 0 and $\hbar$, respectively, and it is better to regard $|F_n\rangle$ as a coherent state of atoms in angular momenta superpositions. The states (3) are mean-field states since the atoms are not entangled. They satisfy

$$a_l|F_n\rangle = \psi_l\sqrt{n}|F_{n-1}\rangle \quad \text{and} \quad a_l a_{l'}|F_n\rangle = \psi_l\psi_{l'}\sqrt{n(n-1)}|F_{n-2}\rangle \tag{4}$$

Because each atom in (3) carries a copy of the qubit state $|\psi\rangle = \psi_0|0\rangle + \psi_1|1\rangle$, the state $|F_n\rangle$ exhibits a bosonic orthogonality catastrophe[39] in the large n limit, meaning that close qubit states $|\psi\rangle$ and $|\psi'\rangle$ encode to orthogonal $|F_n\rangle$ and $|F_n'\rangle$ as $n \to \infty$ (the semiclassical limit in the spin coherent state picture[6]). Furthermore, due to the polynomial encoding in $|F_n\rangle$, the single-particle superposition principle with respect to $\psi_{0,1}$ is violated (see below).

In the atomtronic implementation, we assume a toroidal BEC operated in a regime supporting metastable quantized

circulation states with l trapped vortices

$$|\Phi_l^n\rangle = \frac{(a_l^\dagger)^n}{\sqrt{n}}|\text{vac}\rangle \tag{5}$$

where $a_l^\dagger$ creates an atom in the ring with angular momentum $l \in \mathbb{Z}$. These states are stabilized by the repulsive atomic interactions.[40,41] An atom with mass m and $l = 1$ has velocity $\hbar/mR$ and circles the ring with angular velocity $\Omega_0 = \hbar/mR^2$. We construct a low-energy effective description for the BEC within the manifold of states (3). This is possible because they are selected out by the path integral in the large n limit, due to their diverging contribution to the action. The action in the subspace spanned by these states is

$$S_{\text{eff}}[\bar{\psi}_l, \psi_l] = \int dt \, \langle F_n | i\partial_t - H_{\text{rot}} | F_n \rangle \tag{6}$$

where H_{rot} is the BEC Hamiltonian in the rotating frame. The BEC is rotated with frequency $\Omega \approx \Omega_0/2$ to bring the 0-vortex (no circulation) state $|\Phi_0^n\rangle$ and the 1-vortex state $|\Phi_1^n\rangle$ close in energy. Higher energy l are then neglected, leading to a two-mode model. In the large n limit (see Appendix) the saddle point equations are

$$\frac{d}{dt}\begin{pmatrix}\psi_0\\ \psi_1\end{pmatrix} = -iH_{\text{eff}}\begin{pmatrix}\psi_0\\ \psi_1\end{pmatrix}, \quad H_{\text{eff}} = V_{01}\sigma^x + B_z\sigma^z + g(|\psi_0|^2 - |\psi_1|^2)\,\sigma^z \tag{7}$$

The first two terms in H_{eff} generate rigid x and z rotations of the Bloch sphere. Rotations about x couple $l = 0$ and $l = 1$ angular momenta are produced by breaking rotational symmetry. Here V_{01} is a matrix element for an applied potential energy barrier. The parameter B_z is controlled by the frequency Ω of the BEC rotation discussed above. The nonlinear term describes a z rotation with a rate that increases with increasing Bloch sphere coordinate $\text{tr}(\rho\sigma^z) = |\psi_0|^2 - |\psi_1|^2$, vanishes on the equator, and reverses direction for $\text{tr}(\rho\sigma^z) < 0$. This z-axis torsion[42] (1-axis twisting[43]) of the Bloch sphere is the key to fast state discrimination but is prohibited in ordinary single-particle quantum mechanics. Although the qubit here is informational and not associated with any physical 2-state system, we can define a logical basis $\{|0\rangle, |1\rangle\}$ and treat it like any other qubit:

$$|\psi\rangle = \psi_0|0\rangle + \psi_1|1\rangle = \begin{pmatrix}\psi_0\\ \psi_1\end{pmatrix}, \quad |0\rangle := \begin{pmatrix}1\\ 0\end{pmatrix} = |\Phi_0^n\rangle, \quad |1\rangle := \begin{pmatrix}0\\ 1\end{pmatrix} = |\Phi_1^n\rangle \tag{8}$$

It should be emphasized that (3) is the physical state of the quantum gas, not (8). However the basis states $|0\rangle, |1\rangle$ are the quantized circulation states $|\Phi_{0,1}^n\rangle$, which is important for the readout step.

1.2. Single-Input State Discrimination

As an application, we consider the problem of quantum state discrimination,[44–47] a basic task in quantum information science. In the two-state variant considered here, a quantum state $|\psi\rangle \in \{|a\rangle, |b\rangle\}$ is input to a processor, which knows the values of $|a\rangle$ and $|b\rangle$ ahead of time and tries to determine which was provided (with a bounded failure probability). This is easy if $|a\rangle$ and $|b\rangle$ are orthogonal: For a qubit, a single unitary $U_{\text{read}} = |0\rangle\langle a| + |1\rangle\langle b|$ rotates $\alpha|a\rangle + \beta|b\rangle$ to $\alpha|0\rangle + \beta|1\rangle$, which is then measured on a standard basis. The challenging case is when $|a\rangle$ and $|b\rangle$ are similar, $|\langle a|b\rangle|^2 = 1 - 2^{-k}$ with $k \gg 1$, where $n > 2^k$ identical copies of the input are required.[48] In minimum-error discrimination, the subroutine selects $|a\rangle$ or $|b\rangle$, each with some probability of error, and the objective is to minimize the average error. In unambiguous state discrimination, the subroutine identifies $|a\rangle$ or $|b\rangle$ perfectly, but has the possibility of abstaining, returning an inconclusive result. State discrimination can be used to solve NP-complete (and harder) problems,[29,33,49] at the expense of 2^k input copies and exponential runtime. This cost reflects the limited information gained from measurement.

Abrams and Lloyd[29] showed that certain nonlinearity in the Schrödinger equation would bypass this exponential cost, allowing NP-complete problems to be solved efficiently (in an idealized setting with no errors or decoherence). However, the presence of such nonlinearity would constitute a fundamental modification of quantum mechanics that is not supported by experiments.[50–53] In a condensate, the nonlinearity is not fundamental, but effective. Although we *can* realize nonlinear gates, this does not constitute a complexity violation, due to the large n requirement of mean-field theory.

2. Protocol

The process is illustrated in **Figure 2**. A single state $|\psi\rangle \in \{|a\rangle, |b\rangle\}$ is input to the discriminator, which ideally returns output $|0\rangle$ if $|\psi\rangle = |a\rangle$, or returns $|1\rangle$ if $|\psi\rangle = |b\rangle$. The single-input discriminator regarded as a channel must be nonunitary because the overlap $\langle a|b\rangle$ is not preserved. Equivalently, the distance $\|\rho_a - \rho_b\|_1$ between their density matrices in trace norm is not preserved in time (here $\|X\|_1 := \text{tr}\sqrt{X^\dagger X}$). For pure states, $\|\rho_a - \rho_b\|_1 = 2|\sin(\theta_{ab}/2)|$, where θ_{ab} is the angle between their Block vectors. Linear completely positive trace preserving (CPTP) channels satisfy $\frac{d}{dt}\|\rho_a - \rho_b\|_1 \le 0$; they are either distance preserving or strictly contractive on the inputs.[54] Because the discriminator orthogonalizes the potential inputs, it is *expansive* on those inputs: $\frac{d}{dt}\|\rho_a - \rho_b\|_1 > 0$. Thus, the discriminator is described by a nonlinear PTP channel.[29,36,42]

The implementation proposed here does not discriminate an unknown input (produced by a previous computation), but instead uses a black box state preparation step to randomly prepare $|a\rangle$ or $|b\rangle$, with a small Bloch vector angle $\theta_{ab} \ge 0$ between them. Then $|\langle a|b\rangle|^2 = \cos^2(\theta_{ab}/2) \approx 1 - (\theta_{ab}/2)^2$. This can be accomplished by initializing in the $|\Phi_0^n\rangle$ state and using V_{01} and B_z in (7) to apply x and z rotations. (Ideally, this step is hidden from the remainder of the experiment.) The discrimination gate itself follows refs. [29,33] and uses the z-axis torsion to increase the angle between $|a\rangle$ and $|b\rangle$. It's clear that $|a\rangle$ and $|b\rangle$ should begin with equal and opposite z components $z_a = -z_b$ [here $r_{a,b}^\mu = \text{tr}(\rho_{a,b}\sigma^\mu)$, $\mu \in \{1,2,3\}$]. Consider a simple option with $y_{a,b} = 0$, namely

$$|a\rangle = \cos\left(\frac{\pi - \theta_{ab}}{4}\right)|0\rangle + \sin\left(\frac{\pi - \theta_{ab}}{4}\right)|1\rangle \tag{9}$$

Figure 2. State discrimination channel. Here $\langle a|b\rangle \neq 0$ but $\langle 0|1\rangle = 0$, so the channel must be nonlinear. Note that the output is always a basis state, $|0\rangle$ or $|1\rangle$, simplifying readout.

$$|b\rangle = \cos\left(\frac{\pi+\theta_{ab}}{4}\right)|0\rangle + \sin\left(\frac{\pi+\theta_{ab}}{4}\right)|1\rangle \tag{10}$$

which has

$$x_a = x_b = \left|\cos\left(\frac{\theta_{ab}}{2}\right)\right|, \quad y_a = y_b = 0, \quad z_a = \sin\left(\frac{\theta_{ab}}{2}\right), \quad z_b = -\sin\left(\frac{\theta_{ab}}{2}\right) \tag{11}$$

After switching on g, the two input options evolve as $R_z(\pm g t\theta_{ab})$ and orthogonalize after a time $t \approx \pi/g\theta_{ab}$. However, this implementation does not have a favorable scaling with θ_{ab}. The optimal protocol for nonlinear discrimination was derived by Childs and Young (CY) in [33]. Instead of (11), the CY gate begins with

$$x_a = x_b = \left|\cos\left(\frac{\theta_{ab}}{2}\right)\right|, \quad y_a = z_a = \frac{\sin(\frac{\theta_{ab}}{2})}{\sqrt{2}}, \quad y_b = z_b = -\frac{\sin(\frac{\theta_{ab}}{2})}{\sqrt{2}} \tag{12}$$

and applies x rotations to hold $y_{a,b} = z_{a,b}$ during the subsequent evolution in order to reach antipodal points on the Bloch sphere. The options orthogonalize in a time $t = O(\log \frac{1}{\theta_{ab}})$, after which a readout gate U_{read} (defined with respect to time-evolved $|a\rangle, |b\rangle$) transforms them to circulation states $|\Phi_0^n\rangle$ or $|\Phi_1^n\rangle$, which is then measured via time-of-flight.[55,56]

In an idealized context where (7) is regarded as exact, and where there are no control errors, readout errors, decoherence errors, or noise, the nonlinear discriminator works perfectly every time. We refer to this idealization as a *single-input* discriminator to distinguish it from the more familiar minimum error and unambiguous discriminators based on linear CPTP channels.[44–47] Of course, any actual atomtronic realization is likely to suffer from all such errors and may fail to give the correct answer or return an answer at all. Although the theoretically achievable performance depends sensitively on the system and device details, and is beyond the scope of this work, we note that combining torsion with non-CP dissipation is predicted to implement an *autonomous* discriminator,[36] whose control sequence and operation is (mostly) independent of $|a\rangle$ and $|b\rangle$. In this implementation, the nonlinearity and dissipation create two basins of attraction with a shared boundary in the Bloch ball, one with an attracting fixed point near $|0\rangle$ and the other with an attracting fixed point near $|1\rangle$, giving the discriminator a degree of intrinsic fault tolerance.

The presence of channel nonlinearity indicates a breakdown of the superposition principle. **Figure 3** illustrates a nice example of this effect: In Figure 3a, the evolution of a superposition $\psi_0|0\rangle + \psi_1|1\rangle$ is given by a superposition of evolved basis states $e^{-it}|0\rangle$ and $e^{it}|1\rangle$, shown as a velocity field. However in Figure 3b, the evolved states $e^{-it}|0\rangle$ and $e^{-it}|1\rangle$ are now static (phase factors are a global phase), whereas the actual dynamics are not, except on the equatorial plane.

3. Conclusions

We have discussed an approach to quantum information processing that leverages the special properties of condensates, including their nonlinearity, and proposed an atomtronic implementation of a "nonlinear" qubit. An experimental demonstration of nonlinear state discrimination, while striking, would not by itself constitute a *computation*, because the qubit is not coupled to anything. To implement a useful computation, the BEC qubit must be entangled with other qubits (for example trapped ions) in a scalable circuit-model quantum computer, which is not addressed here.

The standard models of quantum computation assume gates and errors based on linear CPTP channels. Physical hardware, however, might admit initial correlation and be better described by more general maps.[57,58] It is therefore interesting to investigate any additional computational power enabled by quantum channels beyond the linear CPTP paradigm, as we did here. Another example was investigated by Chen et al.,[59] who experimentally demonstrated unambiguous state discrimination in a linear but non-Hermitian optical system. After completing this work, Großardt posted a preprint[8] proposing the use of a two-component BEC coupled to a neutral atom computer to simulate a large family of nonlinear Schrödinger equations. Given their potential for fast quantum state discrimination and simulation of the nonlinear Schrödinger equation, the non-Hermitian and nonlinear approaches to quantum information processing deserve further exploration.

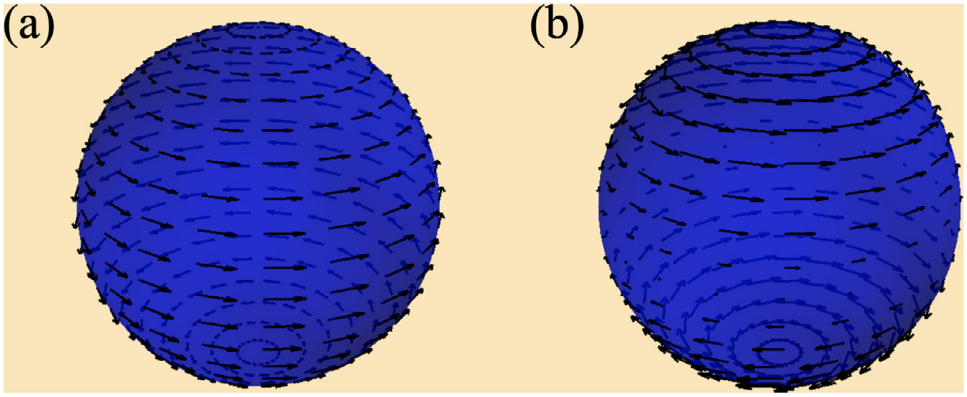

Figure 3. Linear versus nonlinear qubit evolution. a) Unitary evolution. Vectors show the isometric flow of states on the Bloch sphere generated by linear Hamiltonian $H = \sigma^z$. b) Torsion dynamics generated by nonlinear Hamiltonian $H = \langle\psi|\sigma^z|\psi\rangle\,\sigma^z$.

Appendix A: BEC Model

Here we derive the qubit equation of motion (7). We consider a toroidal BEC (thin circular ring with radius R) with rotating tunneling barriers that act as Josephson junctions.[10–12,16] Thin means the dynamics are quasi-1d in the azimuthal direction, θ. This requires the energy, temperature, and effective interaction strength to be below an energy scale $\Delta\epsilon$ determined by the confining potential. The shape of the potential (without barriers) is mostly arbitrary as long as it is invariant under rotations about the axis threading the ring, which we call the z -axis. The angular momentum eigenfunctions on the ring are $\varphi_l(\theta) = e^{il\theta}/\sqrt{2\pi R}$, with $l \in \mathbb{Z}$ the angular momentum. In the absence of tunnel barriers and interaction, these are stationary states. The condensate consists of n weakly interacting bosonic atoms of mass m, each in their electronic ground state $|\Psi_0\rangle$. At sufficiently low energy and density, the atomic collisions are elastic, and the Hamiltonian is

$$H(t) = \int_{\mathrm{Vol}} d^3r \left\{ \frac{\hbar^2 \nabla\phi^\dagger \cdot \nabla\phi}{2m} + \frac{U}{2}\phi^\dagger\phi^\dagger\phi\,\phi + V\phi^\dagger\phi \right\},$$
$$[\phi(\mathbf{r}), \phi^\dagger(\mathbf{r}')] = \delta(\mathbf{r}-\mathbf{r}') \tag{A1}$$

Here Vol is the volume of the ring, $U = 4\pi\hbar^2 a_s/m$ is a short-range interaction strength (proportional to the s-wave scattering length a_s), and $V(\mathbf{r}, t)$ is a confining potential, including the rotating barriers. Acting on the vacuum, $\phi^\dagger(\mathbf{r})$ creates a bosonic atom in state $|\Psi_0\rangle$ at point $\mathbf{r}$. We assume a tunable repulsive interaction with $a_s \geq 0$. We also assume zero temperature, no dissipation, and no disorder.

Two rotating tunnel barriers are used to implement an atomtronic quantum interference device.[11,12] When the barriers are turned on, the Hamiltonian (A1) is time-dependent. Assuming the barriers are rigidly rotated about the z -axis with frequency Ω, we have $V(\mathbf{r}, t) = e^{-i\Omega t L_z/\hbar}\, V(\mathbf{r}, 0)\, e^{i\Omega t L_z/\hbar}$, where L_z is the angular momentum.

However, we can transform to a noninertial reference frame in which the Hamiltonian, H_{rot}, is time-independent. Decomposing the time-evolution operator in the lab frame as

$$U_{\mathrm{lab}} = Te^{-\frac{i}{\hbar}\int_0^t H dt'} = e^{-i\Omega t L_z/\hbar} U_{\mathrm{rot}} \tag{A2}$$

we obtain

$$\frac{dU_{\mathrm{rot}}}{dt} = -\frac{i}{\hbar} H_{\mathrm{rot}} U_{\mathrm{rot}}, \quad H_{\mathrm{rot}} = e^{i\Omega t L_z/\hbar}(H - \Omega L_z)e^{-i\Omega t L_z/\hbar} = H(0) - \Omega L_z \tag{A3}$$

Next we discuss the two-mode limit: In the low energy, thin ring limit, we can expand the field operators and angular momentum as

$$\phi(\mathbf{r}) = \sum_l \frac{e^{il\theta}}{\sqrt{\mathrm{Vol}}} a_l, \quad L_z = \sum_l \hbar l a_l^\dagger a_l, \quad [a_l, a_{l'}^\dagger] = \delta_{ll'} \tag{A4}$$

which leads to

$$H_{\mathrm{rot}} = \frac{\hbar\Omega_0}{2}\sum_l l^2 a_l^\dagger a_l + \frac{U}{2\,\mathrm{Vol}}\sum_{l_1,l_2,l_3} a_{l_1+l_3}^\dagger a_{l_2-l_3}^\dagger a_{l_2} a_{l_1}$$
$$+ \sum_{l_1,l_2} V_{l_1 l_2}\, a_{l_1}^\dagger a_{l_2} - \hbar\Omega \sum_l l a_l^\dagger a_l \tag{A5}$$

where

$$V_{l_1 l_2} = \oint \frac{d\theta}{2\pi} V(\theta, t{=}0)\, e^{-i(l_1-l_2)\theta} \tag{A6}$$

Nonzero $V_{l_1 l_2}$ induce transitions between angular momentum states. Then we have

$$H_{\mathrm{rot}} = \sum_l \hbar\omega_l a_l^\dagger a_l + \frac{U}{2\,\mathrm{Vol}}\sum_{l_1,l_2,l_3} a_{l_1+l_3}^\dagger a_{l_2-l_3}^\dagger a_{l_2} a_{l_1}$$
$$+ \sum_{l_1,l_2} V_{l_1 l_2}\, a_{l_1}^\dagger a_{l_2} - \frac{n\hbar\Omega^2}{2\Omega_0} \tag{A7}$$

where

$$\omega_l = \frac{(\Omega - l\Omega_0)^2}{2\Omega_0}, \quad \omega_0 = \frac{\Omega^2}{2\Omega_0}, \quad \omega_1 = \frac{(\Omega-\Omega_0)^2}{2\Omega_0} \tag{A8}$$

As explained above, the BEC is rotated with frequency $\Omega \approx \Omega_0/2$ to bring the $l = 0$ and $l = 1$ states close in energy. We restrict (A7) to angular momenta $l = 0, 1$ neglecting the others on the basis of their higher energy. Then

$$\sum_{l_1,l_2,l_3} a_{l_1+l_3}^\dagger a_{l_2-l_3}^\dagger a_{l_2} a_{l_1}$$
$$= \sum_{l\in\mathbb{Z}} \left\{ a_l^\dagger a_{-l}^\dagger a_0 a_0 + a_{l+1}^\dagger a_{-l}^\dagger a_0 a_1 + a_l^\dagger a_{1-l}^\dagger a_1 a_0 + a_{1+l}^\dagger a_{1-l}^\dagger a_1 a_1 \right\} \tag{A9}$$

$$= a_0^\dagger a_0^\dagger a_0 a_0 + a_1^\dagger a_1^\dagger a_1 a_1 + 4 a_0^\dagger a_1^\dagger a_1 a_0 \tag{A10}$$

$$= (a_0^\dagger a_0)^2 - a_0^\dagger a_0 + (a_1^\dagger a_1)^2 - a_1^\dagger a_1 + 4 a_0^\dagger a_0 a_1^\dagger a_1 \tag{A11}$$

This leads to a two-mode model

$$H_{\rm rot} = \sum_{l=0,1} \left(\hbar\omega_l + V_{ll} + \gamma a_l^\dagger a_l - \gamma\right) a_l^\dagger a_l + \gamma' a_0^\dagger a_0 a_1^\dagger a_1 + \left(V_{01} a_0^\dagger a_1 + \bar{V}_{01} a_1^\dagger a_0\right) - \frac{n\hbar\Omega^2}{2\Omega_0} \tag{A12}$$

where

$$\gamma = \frac{U}{2\,\mathrm{Vol}}, \quad \gamma' = 4\gamma = \frac{2U}{\mathrm{Vol}} \tag{A13}$$

In what follows we will treat $\gamma, \gamma' \geq 0$ as independent parameters, allowing (A12) to apply to other systems as well. The last term in (A12) subtracts the classical kinetic energy of the spinning ring: $n\hbar\Omega^2/2\Omega_0 = \frac{1}{2} I_{\rm ring}\Omega^2$, $I_{\rm ring} = nmR^2$.

Finally, we discuss the large n limit: Condensates feature an enhanced two-particle interaction $\langle a^\dagger a^\dagger a a\rangle \approx n(n-1)$ caused by the effectively infinite-ranged interaction between condensed atoms. This makes a naive large n limit unphysical, because the energy per particle diverges,[60] and our low-energy assumptions would be violated. The framework discussed here is instead based on a modified large n limit where the interaction simultaneously weakens as $1/n$ (a standard assumption in rigorous studies of mean-field theory[60,61]). This allows for a rigorous study of the large n limit including bounds on the accuracy of mean field theory. For real $V_{01} = \oint \frac{d\theta}{2\pi} V(\theta)\, e^{i\theta}$, and after dropping the classical kinetic energy term (which does not affect the qubit dynamics) we obtain

$$H_{\rm rot} = \sum_{l=0,1} \left((\hbar\omega_l + V_{ll}) a_l^\dagger a_l + \gamma a_l^\dagger a_l^\dagger a_l a_l - \gamma a_l^\dagger a_l\right) + \gamma' a_0^\dagger a_0 a_1^\dagger a_1 + V_{01}\left(a_0^\dagger a_1 + a_1^\dagger a_0\right) \tag{A14}$$

Evaluating (6) and assuming $n \gg 1$ leads to (setting $\hbar = 1$)

$$S_{\rm eff} = n\int dt \left\{ \sum_{l=0,1} \left(\bar{\psi}_l i\partial_t \psi_l - (\omega_l + V_{ll})|\psi_l|^2 - n\gamma\,|\psi_l|^4\right) - n\gamma'|\psi_0\psi_1|^2 - V_{01}(\bar{\psi}_0\psi_1 + \bar{\psi}_1\psi_0)\right\} \tag{A15}$$

Here $\bar{z}$ denotes complex conjugation. Due to the $O(n^2)$ interaction energies in (A14), we cannot take the $n \to \infty$ limit in (A15) without violating our low-energy assumptions. Instead, we consider a modified limit defined by the simultaneous limits $\gamma, \gamma' \to 0$, $n \to \infty$, and low energy. To evaluate (A15) in this limit we assume that the interaction strengths decrease with n as $\gamma = K/n$ and $\gamma' = K'/n$, where K and K' are now fixed coupling constants. Then

$$S_{\rm eff} = n\int dt \left\{ \sum_{l=0,1} \left(\bar{\psi}_l i\partial_t \psi_l - (\hbar\omega_l + V_{ll})|\psi_l|^2 - K|\psi_l|^4\right) - K'|\psi_0\psi_1|^2 - V_{01}(\bar{\psi}_0\psi_1 + \bar{\psi}_1\psi_0)\right\} \tag{A16}$$

To obtain (A16) we have used the results summarized below in **Table** A1, which also gives the corresponding results for encoding (2). In the large n limit the stationary phase approximation leads to (7) with

Table A1. One- and two-particle correlators versus encoding.

	$\langle a_l^\dagger a_{l'}\rangle$	$\langle a_l^\dagger a_l a_{l'}^\dagger a_{l'}\rangle$
$\lvert \mathrm{CAT}_n\rangle$	$n\,\lvert\psi_l\rvert^2\delta_{ll'}$	$n(n-1)\,\lvert\psi_l\rvert^2\delta_{ll'}$
$\lvert F_n\rangle$	$n\,\psi_l^*\psi_{l'}$	$n(n-1)\,\lvert\psi_l\rvert^2\lvert\psi_{l'}\rvert^2$

$$H_{\rm eff} = \begin{pmatrix} \hbar\omega_0 + V_{00} + 2K|\psi_0|^2 + K'\,|\psi_1|^2 & V_{01} \\ V_{01} & \hbar\omega_1 + V_{11} + 2K|\psi_1|^2 + K'\,|\psi_0|^2 \end{pmatrix} \tag{A17}$$

$$= V_{01}\sigma^x + B_z\sigma^z + g\,\mathrm{tr}(\rho\sigma^z)\,\sigma^z + \mathrm{const.} \tag{A18}$$

where

$$B_z := \frac{\hbar\omega_0 - \hbar\omega_1 + V_{00} - V_{11}}{2} \quad \text{and} \quad g := \frac{2K - K'}{2} = -\frac{Un}{2\,\mathrm{Vol}} \tag{A19}$$

This concludes the derivation of (7).

Acknowledgements

This work was partly supported by the NSF under grant no. DGE-2152159.

Conflict of Interest

The authors declare no conflict of interest.

Data Availability Statement

Data sharing is not applicable to this article as no new data were created or analyzed in this study.

Keywords

atomtronic squids, nonlinear master equations, quantum state discrimination

Received: December 5, 2023
Revised: April 24, 2024
Published online: May 5, 2024

[1] L. Amico, M. Boshier, G. Birkl, A. Minguzzi, C. Miniatura, L.-C. Kwek, D. Aghamalyan, V. Ahufinger, D. Anderson, N. Andrei, A. S. Arnold, M. Baker, T. A. Bell, T. Bland, J. P. Brantut, D. Cassettari, W. J. Chetcuti, F. Chevy, R. Citro, S. De Palo, R. Dumke, M. Edwards, R. Folman, J. Fortagh, S. A. Gardiner, B. M. Garraway, G. Gauthier, A. Günther, T. Haug, C. Hufnagel, et al., *AVS Quantum Sci.* **2021**, *3*, 039201.
[2] L. Amico, D. Anderson, M. Boshier, J.-P. Brantut, L.-C. Kwek, A. Minguzzi, W. von Klitzing, *Rev. Mod. Phys.* **2022**, *94*, 041001.
[3] J. I. Cirac, M. Lewenstein, K. Mølmer, P. Zoller, *Phys. Rev. A* **1998**, *57*, 1208.
[4] L. Tian, P. Zoller, *Phys. Rev. A* **2003**, *68*, 042321.
[5] T. Byrnes, K. Wen, Y. Yamamoto, *Phys. Rev. A* **2012**, *85*, 040306(R).

[6] T. Byrnes, D. Rosseau, M. Khosla, A. Pyrkov, A. Thomasen, T. Mukai, S. Koyama, A. Abdelrahman, E. Ilo-Okeke, *Opt. Commun.* **2015**, *337*, 102.
[7] F. S. Luiz, E. I. Duzzioni, L. Sanz, *Braz. J. Phys.* **2015**, *45*, 550.
[8] A. Großardt, Nonlinear-ancilla aided quantum algorithm for nonlinear Schrödinger equations, arXiv: 2403.10102.
[9] D. Solenov, D. Mozyrsky, *J. Comput. Theor. Nanosci.* **2011**, *8*, 481.
[10] L. Amico, D. Aghamalyan, F. Auksztol, H. Crepaz, R. Dumke, L. C. Kwek, *Sci. Rep.* **2014**, *4*, 4298.
[11] D. Aghamalyan, N. T. Nguyen, F. Auksztol, K. S. Gan, M. M. Valado, P. C. Condylis, L.-C. Kwek, R. Dumke, L. Amico, *New J. Phys.* **2016**, *18*, 075013.
[12] C. Ryu, E. C. Samson, M. G. Boshier, *Nat. Commun.* **2020**, *11*, 3338.
[13] K. T. Kapale, J. P. Dowling, *Phys. Rev. Lett.* **2005**, *95*, 173601.
[14] C. Ryu, M. F. Andersen, P. Cladé, V. Natarajan, K. Helmerson, W. D. Phillips, *Phys. Rev. Lett.* **2007**, *99*, 260401.
[15] A. Ramanathan, K. C. Wright, S. R. Muniz, M. Zelan, W. T. Hill III, C. J. Lobb, K. Helmerson, W. D. Phillips, K. C. Gampbell, *Phys. Rev. Lett.* **2011**, *106*, 130401.
[16] S. Eckel, J. G. Lee, F. Jendrzejewski, N. Murray, C. W. Clark, C. J. Lobb, W. D. Phillips, M. Edwards, G. K. Campbell, *Nature* **2014**, *506*, 200.
[17] H. Kim, G. Zhu, J. V. Porto, M. Hafezi, *Phys. Rev. Lett.* **2018**, *121*, 133002.
[18] L. Pezzè, K. Xhani, C. Daix, N. Grani, B. Donelli, F. Scazza, D. Hernandez-Rajkov, W. J. Kwon, G. Del Pace, G. Roati, Stabilizing persistent currents in an atomtronic Josephson junction necklace, arXiv: 2311.05523.
[19] S. A. Moses, C. H. Baldwin, M. S. Allman, R. Ancona, L. Ascarrunz, C. Barnes, J. Bartolotta, B. Bjork, P. Blanchard, M. Bohn, J. G. Bohnet, N. C. Brown, N. Q. Burdick, W. C. Burton, S. L. Campbell, J. P. Campora, C. Carron, J. Chambers, J. W. Chan, Y. H. Chen, A. Chernoguzov, E. Chertkov, J. Colina, J. P. Curtis, R. Daniel, M. DeCross, D. Deen, C. Delaney, J. M. Dreiling, C. T. Ertsgaard, et al., *Phys. Rev. X* **2023**, *13*, 041052.
[20] S. Krinner, N. Lacroix, A. Remm, A. Di Paolo, E. Genois, C. Leroux, C. Hellings, S. Lazar, F. Swiadek, J. Herrmann, G. J. Norris, C. K. Andersen, M. Müller, A. Blais, C. Eichler, A. Wallraff, *Nature* **2022**, *605*, 669.
[21] Google Quantum AI, *Nature* **2023**, *614*, 676.
[22] D. C. McKay, I. Hincks, E. J. Pritchett, M. Carroll, L. C. G. Govia, S. T. Merkel, Benchmarking quantum processor performance at scale, arXiv: 2311.05933.
[23] D. Bluvstein, H. Levine, G. Semeghini, T. T. Wang, S. Ebadi, M. Kalinowski, A. Keesling, N. Maskara, H. Pichler, M. Greiner, V. Vuletić, M. D. Lukin, *Nature* **2022**, *604*, 451.
[24] T. M. Graham, Y. Song, J. Scott, C. Poole, L. Phuttitarn, K. Jooya, P. Eichler, X. Jiang, A. Marra, B. Grinkemeyer, M. Kwon, M. Ebert, J. Cherek, M. T. Lichtman, M. Gillette, J. Gilbert, D. Bowman, T. Ballance, C. Campbell, E. D. Dahl, O. Crawford, N. S. Blunt, B. Rogers, T. Noel, M. Saffman, *Nature* **2022**, *604*, 457.
[25] V. Coffman, J. Kundu, W. K. Wootters, *Phys. Rev. A* **2000**, *61*, 052306.
[26] X.-L. Zong, H.-H. Yin, W. Song, Z.-L. Cao, Monogamy of quantum entanglement, arXiv: 2201.00366.
[27] E. P. Gross, *Nuovo Cimento* **1961**, *20*, 454.
[28] L. P. Pitaevskii, *Sov. Phys. JETP* **1961**, *13*, 451.
[29] D. S. Abrams, S. Lloyd, *Phys. Rev. Lett.* **1998**, *81*, 3992.
[30] B. Wu, Q. Niu, *Phys. Rev. A* **2000**, *62*, 023402.
[31] M. F. Riedel, P. Böhi, Y. Li, T. W. Hänsch, A Sinatra, P. Treutlein, *Nature* **2010**, *464*, 1170.
[32] D. A. Meyer, T. G. Wong, *New J. Phys.* **2013**, *15*, 063014.
[33] A. M. Childs, J. Young, *Phys. Rev. A* **2016**, *93*, 022314.
[34] S. Xu, J. Schmiedmayer, B. C. Sanders, *Phys. Rev. Res.* **2022**, *4*, 023071.
[35] S. Deffner, *Europhys. Lett.* **2022**, *140*, 48001.
[36] M. R. Geller, Adv. Quantum Technol. **2023**, 2200156, arXiv: 2111.05977.
[37] L. Erdős, B. Schlein, *J. Stat. Phys.* **2009**, *134*, 859.
[38] M. R. Geller, Phys. Rev. A **2023**, *108*, 042210, arXiv: 2112.09005.
[39] N.-E. Guenther, R. Schmidt, G. M. Bruun, V. Gurarie, P. Massignan, *Phys. Rev. A* **2021**, *103*, 013317.
[40] E. J. Mueller, *Phys. Rev. A* **2002**, *66*, 063603.
[41] S. Baharian, G. Baym, *Phys. Rev. A* **2013**, *87*, 013619.
[42] B. Mielnik, *J. Math. Phys.* **1980**, *21*, 44.
[43] M. Kitagawa, M. Ueda, *Phys. Rev. A* **1993**, *47*, 5138.
[44] S. M. Barnet, S. Croke, Quantum state discrimination, arXiv: 0810.1970.
[45] J. Bae, W.-Y. Hwang, *Phys. Rev. A* **2013**, *87*, 012334.
[46] J. Bae, L.-C. Kwek, *J. Phys. A: Math. Theor.* **2015**, *48*, 083001.
[47] M. Rouhbakhsh, S. A. Ghoreishi, Minimum-error discrimination of qubit states revisited, arXiv: 2108.12299.
[48] C. W. Helstrom, *Quantum Detection and Estimation Theory*, Academic Press, Cambridge, MA **1976**.
[49] S. Aaronson, NP-complete problems and physical reality, arXiv: quant-ph/0502072.
[50] J. J. Bollinger, D. J. Heinzen, W. M. Itano, S. L. Gilbert, D. J. Wineland, *Phys. Rev. Lett.* **1989**, *63*, 1031.
[51] T. E. Chupp, R. J. Hoare, *Phys. Rev. Lett.* **1990**, *64*, 2261.
[52] R. L. Walsworth, I. F. Silvera, E. M. Mattison, R. F. C. Vessot, *Phys. Rev. Lett.* **1990**, *64*, 2599.
[53] P. K. Majumder, B. J. Venema, S. K. Lamoreaux, B. R. Heckel, E. N. Fortson, *Phys. Rev. Lett.* **1990**, *65*, 2931.
[54] M. B. Ruskai, *Rev. Math. Phys.* **1994**, *6*, 1147.
[55] L. Amico, A. Osterloh, F. Cataliotti, *Phys. Rev. Lett.* **2005**, *95*, 063201.
[56] S. Moulder, S. Beattie, R. P. Smith, N. Tammuz, Z. Hadzibabic, *Phys. Rev. A* **2012**, *86*, 013629.
[57] J. M. Dominy, A. Shabani, D. A. Lidar, *Quantum Inf. Process.* **2016**, *15*, 465.
[58] J. M. Dominy, D. A. Lidar, *Quantum Inf. Process.* **2016**, *15*, 1349.
[59] D.-X. Chen, Y. Zhang, J.-L. Zhao, Q.-C. Wu, Y.-L. Fang, C.-P. Yang, F. Nori, Quantum state discrimination in a PT-symmetric system, arXiv: 2209.02481.
[60] E. H. Lieb, R. Seiringer, J. Yngvason, *Phys. Rev. A* **2000**, *61*, 043602.
[61] N. Benedikter, M. Porta, B. Schlein, *Effective Evolution Equations from Quantum Dynamics*, Springer, Berlin **2016**.